ASTRO-H

INSTRUMENT CALIBRATION REPORT
SXS TIMING COEFFICIENTS
ASTH-SXS-CALDB-COEFTIME

Version 2.1

29 August 2016

ISAS/ GSFC

Prepared by: M. Tashiro, S. Koyama, C. Kilbourne, F. S. Porter, Y. Kato, S. Takeda, S. Kubota, S. Yamada, and M. Sawada

Table of Contents

CHANGE RECORD PAGE (1 of 1)

DOCUMENT TITLE : SXS Timing Coefficients			
ISSUE	DATE	PAGES AFFECTED	DESCRIPTION
Version 0.2	March 2016	All	First Release
Version 2.1	August 2016	All	Second Release

1. Introduction

1.1 Purpose

The SXS events are classified in pixel event ITYPEs (0, 1, 2, 3, 4, 5, 6, 7) = TYPEs (Hp, Mp, Ms, Lp, Ls, BL, LO, Rj) and anti-co events (see SXS document). Among them, the photon events are Hp through Ls and they are categorized in three "major" type of H (Hp), M (Mp and Ms), and L (Lp and Ls). The first two (H and M) of events are time assigned through the optimal filtering process implemented in the flight software onboard the PSP. Since the L (Lp and Ls) events and anti-co events skip the filtering process, theytheyare tagged with a hardware-determined local time counter (at DERIV_MAX time for L and at the trigger threshold for anti-co). The TYPE = BL events are not photon events and need no time correction with this CALDB file. The TYPEs LO (= lost count event) and Rj (= reject) employ different format and need not to be time assigned in the process, either.

1.2 Scientific Impact

This file contains various time coefficients related to above pixel events of TYPEs, antico detector events and MXS events. Its structure is an empty primary header with 2 extensions. The first extension consists of 12 columns. The first one is TIME. The following 3 columns define time intervals for *sxssecid* task to determine pixel event TYPEs if the re-grade option is set to yes, while the rest define parameters for *sxsflagpix* to flag events indicating coincidence among pixel, anti-co, or MXS events. The second extension describes parameters to re-calculate photon arrival time compensating TYPE, energy, and rise-time of event pulses. Details of these parameters are described in section 2.

2 Release CALDB 20160715

Filename	Valid data	Release data	CALDB Vrs	Comments
ah_sxs_coeftime_20140101v002.fits	2014-01-01	20160715	004	

2.1 Data Description of the first extension: DELTIMES

This extension consists of the following 12 columns, all with units of seconds. The TIME column defines the time when the coefficients in that row become applicable.

The 3 columns after TIME are used by the *sxssecid* task for identifying the primary event associated with a given secondary event, and in event re-grading. The values are defined by onboard software parameters. DTPRIMARY column stores the time interval that distinguishes primary from secondary events (based on the time from the preceding event). The DTLOWMID column stores the time interval that distinguishes low ("major" pixel event type L) from mid-resolution (M) events,, and DTMIDHIGH column stores the time interval that distinguishes high

(H) from mid-resolution (M) events (both based on the time to the nearest event, whether preceding or following).

The following 8 columns are for defining the window used for antico flagging by the *sxsflagpix* task, which determines the time interval of pixel event discrimination with the anti-coincidence with the antico events, pixel cross-talk events or MXS photons.
The ANTSHIFT column stores the time offset between event time and central anti-co time, while the ANTDTPRE column stores the time interval preceding the time of an antico event (shifted by ANTSHIFT) used to define the lower limit of the window, and the ANTDTFOL column stores the time interval following the time of an antico event (shifted by ANTSHIFT) used to define the upper limit of the window. The ANTSHIFT column has two values for each row to accept different values for the two sides of the PSP.

The CTRECDT column stores the time interval that identifies background events originating from cal-pixel recoil electrons. Events occurring within CTRECDT of a cal-pixel event may be flagged by *sxsflagpix*. PROXDT is similar, but applies to any two pixels, in order to flag tightly correlated pairs of background events, such as from an electron lost from one pixel and absorbed by another. The reason to distinguish them is that pairs involving the cal pixel are primarily due to cal-source x-rays, thus the pulses are similar and the dispersion in event timing is small. Thus, if the acceptance window for other pairs needs to be expanded to include the full range of events, it could be restricted for cal-pixel pairs to control the number of false coincidences.

The CTELDT column stores the time interval between events required for electrical crosstalk to be flagged by *sxsflagpix*. This is for the purpose of identifying crosstalk events that have triggered. The CTEL2DT column stores the time interval between events that could be contaminated by untriggered electrical crosstalk. Both of these apply only to pairs of electrical nearest neighbors. Thus, if a small, fast event on pixel 2 occurs within CTELDT of a normal pulse on pixel 3, then pixel 2 would be provisionally flagged as electrical crosstalk. (In practice, the size and rise time should be sufficient to identify it as such.) If events on pixel 2 and pixel 3 occur within CTEL2DT of each other, both events will be flagged because the energy assignment of both events may be contaminated.

The MXSDT column stores the time interval by which the MXS pulse stop times given in the MXS GTI are extended to account for MXS afterglow in flagging events for coincidence with MXS operation in *sxsflagpix*.

2.1.1 evaluation of values: DELTIMES

The values for DTPRIMARY, DTLOWMID, and DTMIDHIGH are intended to match parameter used in the PSP. No study was required for their determination.

Cosmic ray events observed on May 18, June 21, and June 25, 2015 and in orbit (during SXI calibration with RXJ 1856.5–3754 on March 17, 2016) were used to characterize anti-co timing relative to the calorimeter pixels.

Background data from June 21, 2015 were used to characterize the time intervals between correlated pairs of calorimeter events and the results were re-evaluated with the in-orbit RXJ 1856.5-3754 observation data with the revised ARRCOEFS (section 2.2.3). The in-orbit observation was just background for the SXS, since the soft output of RXJ 1856.5-3754 was not transmitted by the Be window of the SXS gate valve.

Low threshold data from May 19, 2015 were used for initial study of the timing of electrical crosstalk. This analysis was re-evaluated with the in-orbit background data from the March 17, 2016 observation of RXJ 1856.5–3754 and the March 25, 2016 observation of the Crab. The dependence of pulse-height determination of a pulse contaminated by undetected electrical crosstalk on the separation in time of that crosstalk was determined by modeling and verified via analysis of MXS data (e.g. in the “Nominal operations test” and FNC-D on November 10-11, 2015).

2.1.2 results: DELTIMES

Cosmic ray events observed on ground show a distribution of time intervals between the trigger times of array events and of their associated anti-co events peaks at 200 ± 40 micro-s, except pixel 26, which peaks 130 micro-s later. The difference for pixel 26 is eliminated with the conversion from SAMPLECNTTRIG to SAMPLECNT (see next section). The systematic difference between pixel and anti-co trigger times is due to the different triggering schemes; the assigned anti-co times are later. The distribution is slightly asymmetric towards longer delays. A range of 40 micros-s to 440 micro-s (relative to the pixel time) covered the distribution in the ground background data. We have to note the shift is determined in reference to SAMPLECNT before correction by ARRCOEFFs.

The in-orbit photon event TIME is determined after being corrected with ARRCOEFFs described in 2.2. Therefore we re-evaluated the ANTISHIFT parameter time intervals between the corrected event TIME and the trigger times of associated anti-co events. Utilizing in-orbit background data, we observed time range of anti-co events distributed between –850 micro-s and –250 micro-s and peaked at around –530 micro-s. The systematic difference from the ground calibration is explained by the effect of newly defined ARRCOEFF parameter b and c summarized in section 2.2.3. To cover the distribution with added margin (a range from –1000 micro-s to 0 micro-s), we determined three parameters, as ANTDTPRE = ANTDTFOL = 500 micro-s and ANTSHIFT = – 500 micro-s (for the both sides of the PSP).

Prior to launch, to study pixel-pixel correlations not involving electrical crosstalk, background data taken with a high PSP threshold (120) was analyzed, and all events with $E < 100$ eV were ignored. The most probable time interval of correlated pairs (looking at all pairs closer than 1.5 ms) was 0, with a standard deviation of 38 micro-s. Given the limited statistics in ground background data, we did not separate pairs involving the cal-pixel from those that did not, and we set CTRECDT = PROXDT = 240 micro-s to cover an integral number (3) of time samples. However, in orbit, we observed a new population of correlated events, similar to the frame events of Suzaku/XRS, apparently due to cosmic-ray interaction in the thick silicon around the array. Many of these events could be rejected based on the value of their rise times, but not all.

In order to reject them by coincidence, we needed to set PROXDT = 720 micro-s, but we left CTRECDT = 240 micro-s to minimize false coincidence with the calibration-source photons.

To study timing offsets to electrical crosstalk, data taken with a low PSP threshold (~25) were analyzed , and correlated pairs involving electrical nearest-neighbor channels were studied. The source x-rays were predominantly Mn K x-rays from ^{55}Fe, with some channels also seeing Cu K x-rays from the MXS. Because the shape of crosstalk is very different from thermal pulses, the time assignment is not robust. Relative to the primary event, crosstalk would need to be flagged within the window of – 640 to +240 micro-s. (Crosstalk from the anti-co into channels 17 and 35 would need an exclusion window of – 1600 to +400 micro-s, relative to anti-co pulse times, which is very different from ordinary anti-co screening.) However, timing is not needed to identify electrical crosstalk. Crosstalk appears at shorter risetimes than normal pulses, and smaller PH values. The gain scales of all grades map electrical crosstalk pulses from x-ray events to energies below 100 eV. Thus energy discrimination easily removes most crosstalk, and risetime discrimination will remove rare crosstalk events from unusually large events. Thus the plan for early operation is not to attempt to identify individual crosstalk pulses, and CTELDT has been set to 1000 micro-s as a placeholder. Further investigation using in-orbit data from the March 17, 2016 observation of RXJ 1856.5-3754 and the March 25, 2016 observation of the Crab confirmed that 1000 micro-s was a good value for CTELDT if electrical crosstalk were to be identified by timing, but also validated the approach of eliminating electrical cross talk by discarding low-energy events. From the Crab data, we determined that we needed to raise that low-energy cut-off to 300 eV to exclude crosstalk events with the L grade. The use of PH to remove crosstalk events makes it possible to use pixel-to-pixel correlation to remove the frame-event clusters.

Undetected crosstalk needs additional consideration. The presence of a crosstalk pulse on an x-ray pulse will alter the energy that the PSP determines for that pulse. Computing the impact of the crosstalk from an 8 keV x-ray on a normal x-ray pulse as a function of displacement from the arrival time of the x-ray event, we determined that the error could be kept to < 0.5 eV if the coincidence window of ±25 ms for electrical nearest neighbors was excluded, with the exception of a very small window of enhancement if a crosstalk pulse arrives in the last 2 ms of a pulse record, due to non-zero power in the filter at the end of the template. The results of this modeling agree with MXS data, for which the pulsed output increases the probability of pulses occurring on adjacent pixels within the pulse time. Thus we set CTEL2DT = 25 ms.

The time scale of the MXS afterglow was measured in many data sets, most extensively in the "Nominal operations test" and FNC-D on November 10-11, 2015. The decay time of the afterglow is characterized by two time constants: 0.6 ms and 4.5 ms. The required waiting time is set by the background requirement, but the relationship between that requirement and MXSDT depends on how the MXS will be used in orbit. We have set MXSDT at 21 ms based on a worst-case operation scenario.

2.1.3 summary of the first extension: DELTIMES

DTPRIMARY = DTMIDHIGH = 69.92 ms

.

DTLOWMID = 17.52 ms
ANTDTPRE = ANTDTFOL = 0.50 ms
ANTSHIFT = –0.50ms (common to PSP-A/B; anti-co time is LATER than calorimeter event)
CTRECDT = 0.24 ms
PROXDT = 0.72 ms
CTELDT = 1 ms (placeholder, not expected to be used)
CTEL2DT = 25 ms
MXSDT = 21 ms

2.2 Data Description of the second extension: ARRCOEFFS

As described in "ASTRO-H Time assignment system (ASTH-SCT-021)", photon arrival time of SXS is calculated from the trigger time or derivative maximum time tagged to each event data. However, methods of trigger time or derivative maximum time determination are different between event grades – "TYPEs", and hence there are to be systematic differences between "TYPEs". The second extension describes the parameters to compensate the discrepancy.

The photon arrival time (TIME) of the SXS instrument are determined by the *ahtime* task using the LOCAL_TIME counter "SAMPLECNT" which is determined by the *sxssamcnt* task as follows (subsection 6.2.4 in ASTH-SCT-021),

SAMPLECNT = SAMPLECNTTRIG – a * (0.25 * RISE_TIME) – b * DERIV_MAX – c.

The parameter set (a, b, c) is defined for each major TYPE (H, M, L) as described above. The corresponding columns in CALDB are AH, AM, AL for the parameter a, BH, BM, BL for the parameter b, and CH, CM, CL for the parameter c. They are stored in units of SAMPLECNT (80 micro-s). In total, 10 columns are defined including the TIME column to specify an applicable time interval for each row. Each of the columns AH through CL stores 36 values for each row to accept pixel dependence of the time coefficients.

2.2.1 evaluation of parameters: ARRCOEFFS

PIXEL, RISE_TIME, DERIV_MAX dependence
Systematic time difference associated with pixel number, event pulse rise time and derivative peak defined in this CALDB file are determined by analysis of cosmic ray events observed on June 21 and 25, 2015 and FW ^{55}Fe events observed on June 25, 2015. For the cosmic-ray data, pixel events associated with anti-co events (within a 1.5 ms time window) were identified, and the relative time differences from the anti-co event were evaluated. For the ^{55}Fe data, ~ 100 pulse dumps were analyzed from each channel. The derivative of each pulse dump was calculated using the PSP algorithm and the time of derivmax was determined and compared with the time assigned to the associated H event. This method allows systematic comparison of H and L time assignments for the same pulse. In principle, it is expected that the time delay of the triggering time depends on the rise time (and pulse height) of each event pulse. However, the difference of raw pulse shape is convolved by the BOXCAR filter and is expected to be small. We saw cosmic-ray event time distribution in reference to event RISE_TIME or DERIV_MAX.

Although we saw small dependence both on RISE_TIME and DERIV_MAX in the range up to 50 keV, it is not significant below 12 keV event. Therefore, in the last version of CALDB, we ignored the RISE_TIME dependence (parameter a) and pulse-height (which is approximately in proportion to the DERIV_MAX) dependence (parameter b). In this version of CALDB, we re-evaluated those dependence with data from Crab pulsar. Although we successfully obtained pulsed light curves with all pixels, the difference was not significant. Therefore. we safely ignore the PIXEL dependence even in this version of CALDB except pixel 26 as described in 2.2.2.

TYPE dependence
ITYPE dependence defined in the last CALDB file was determined by analysis of data obtained in Spacecraft integration test in 2015. The data where from observations taken on SXS-MXS irradiation test in the ASTRO-H integration tests: SXS comprehensive test on 19 May 2015, system function test (FNC-D) in 21 – 22 May 2015 and thermal vacuum test (TVT) in 26 – 27 June 2015. Since the gate valve (GV) was shut during the test, 27 of 35 pixels are shaded by the structure of GV. The values are revised in this CALDB file based on the in orbit calibration data from Crab pulsar. All of pixels detected the pulsation in the orbit. Although the difference in pixels is not evaluated due to the limitation of statistics.

All the data were analyzed with the FTOOLs xronos version 5.22. We extracted pixel event data observed during the MXS periodic pulse irradiation and carried out folding analysis of each pixel or each TYPE events using "efsearch" and "efold". In the analysis of the on-ground calibration with MXS, the start and end times of pulses are recorded in HK data of SXS-MXS (HK_SXS_FWE extension in SXS HK1) and the period and length were set (PLS_SPAC, PLS_LEN) = (78.125 ms, 15.875 ms) for SXS comprehensive & FNC-D or = (62.500 ms, 5.000 ms) for TVT. We evaluate the time epoch and derived phase shift in folded light curve of each TYPE irradiated pixel and determine the rising phase to determine the time shift from the rise time of MXS pulse. In the orbit, we folded the light curve from the Crab pulsar to re-evaluate parameters a, b, and c for the 35 pixels and anti-co data.

2.2.2 Results: ARRCOEFFS

As mentioned in the last version, there we saw no difference in the observed time delay between "primary" and "secondary" events. We therefore summarized the ARRCOEFFs parameters for three "major" event types, H (Hp), M (Mp and Ms), and L (Lp and Ls) in this CALDB file.

Difference in pixels
In contrast with the other pixels, the computed difference between H/M and L timing for pixel 26 was 800 micro-s instead of 930 micro-s. Additionally, for every pixel except pixel 26, the distribution of trigger time offsets from each associated anti-co event time peaks at – (200 ± 40) micro-s. However, the offset of pixel 26 is 130 micro-s later. The PSP uses tickshift to assign a trigger time that is independent of changes to the trigger threshold, but the time of that assignment relative to the true onset of the pulse remains dependent on the thresholds used at the time the optimal filter was computed. A higher threshold was used for pixel 26 due to its high-frequency ringing; thus the time reference for pixel 26 is later than for the other channels (and

thus closer to the time determined at DERIV_MAX). This timing offset for pixel 26 is to be compensated by parameter ‘c’. No significant offset was observed neither in orbit calibration, except for the pixel 26 mentioned above.

Difference in DERIV_MAX

We ignore the RISE_TIME dependence explicitly because of following two reasons. (1) The observed distribution of RISE_TIME are narrow enough and photon events are safely extracted from the criterion of 40 < RISE_TIME < 60 employed in the standard screening process. (2) RISE_TIME of photon events are well correlated with DERIV_MAX values, which implies DERIV_MAX value correction inevitably compensates the implicit RISE_TIME dependence. Therefore we set the parameter a to be zero, and derived parameter b’s for each major TYPEs, using the Crab pulse data as follows,

b_H = –(1.563 ± 1.171)E-04,

b_M = –(1.048 ± 0.886)E-04,

b_L = –(3.329±0.924)E-04.

Each parameter is consistent with data observed in ground tests.

Difference of parameter ‘c’ in TYPEs

As described in the last version based on the on ground tests, we observed time delay from the expected MXS irradiation on time were, 450±30 micro-s and (1360±30) micro-s for TYPEs H & M and TYPE L, respectively. Although we were not able to determine instrumental response time of MXS in the on ground calibration tests, the TYPE to TYPE difference was able to be evaluated for all 36 pixels using H-type events with PSP-assigned times and comparing with L-type times computed from the derivatives of the associated pulse dumps. The obtained relative time difference between TYPE=H/M and TYPE=L is (930±25) micro-s, except for pixel 26, as discussed in the next section.

These delays are approximately explained as below. The obtained absolute value of time difference were determined from the time of LED ON command, although there is a certain response time (~ 1 ms or less) for MXS to radiate X-rays. On the other hand, since the TYPE=H/M event time is determined at the event threshold crossing time of pulse derivative, it is ahead of raw pulse rise by about DERIV_HALF_LEN (half length of the BOXCAR filter = 640 micro-s). Therefore a fixed time delay is reasonable, but with this experiment only the relative time difference of TYPE=H/M and TYPE=L of (910±30) micro-s is reliable to adopted in CALDB data. The time difference is reasonable since TYPE L event time corresponds to DERIV_MAX time which is expected to delay by the full length of the BOXCAR filter = 1280 micro-s minus the time between onset and triggering. Simulations of calorimeter pulses filtered by the Xbox anti-aliasing filter, digitized to 80 micro-s samples, and differentiated by the PSP indicate that for the trigger levels used at the time the optimal filter was generated, the reported trigger time is within a sample of the true arrival time.

Then in this version, we measure the absolute offset time for each TYPE using the Crab pulsar data. We re-evaluate the absolute time offset parameter ‘c’ for each TYPE after time correction using parameter ‘a’ (though it is zero), and ‘b’ as described above. The in-orbit calibration source Crab pulsar exhibits two peaks in a period of ~ 33 ms both in radio and X-ray band, but it

is reported that the first X-ray pulse peak leads the first radio peak by 315 micro-s (Molkov et al. 2010). We employed the coordinate of Crab pulsar of (RA, DEC) =(83.6332, 22.0145) to make geocentric correction, and absolute timing of radio pulse according to Jodrell Bank Crab pulsar timing results – monthly ephemeris. We evaluated the time offset for each TYPE by comparing the obtained first peaks with the expected pulse phase. As results, the time offset of each TYPE of events are,
For pixel 26:
c_H = (547 ± 16) micro-s,
c_M = (558 ± 11) micro-s,
c_L = (1384 ± 11) micro-s.

For other pixels;
c_H = (417 ± 16) micro-s,
c_M = (428 ± 11) micro-s,
c_L = (1384 ± 11) micro-s.

2.2.3 Summary of the second extension: ARRCOEFFS

RISE_TIME dependence is negligible,
a = 0.
Thus, AH = AM = AL = 0 and for all pixels.

DERIV_MAX dependence are observed as,

BH = –1.563E-04
BM = –1.048E-04
BL = –3.329E-04
for all pixels.

TYPE dependence c in the unit of ‘SAMPLECNT (80 micro-s)’ is determined as,
For pixel 26;
CH = 6.840
CM = 6.970
CL = 17.296.

For the other pixels;
CH = 5.215
CM = 5.345
CL = 17.296.

3 Comparison with the previous release

This is the second and last release revised with the in orbit calibration data. The difference from the last version is summarized in figure below.

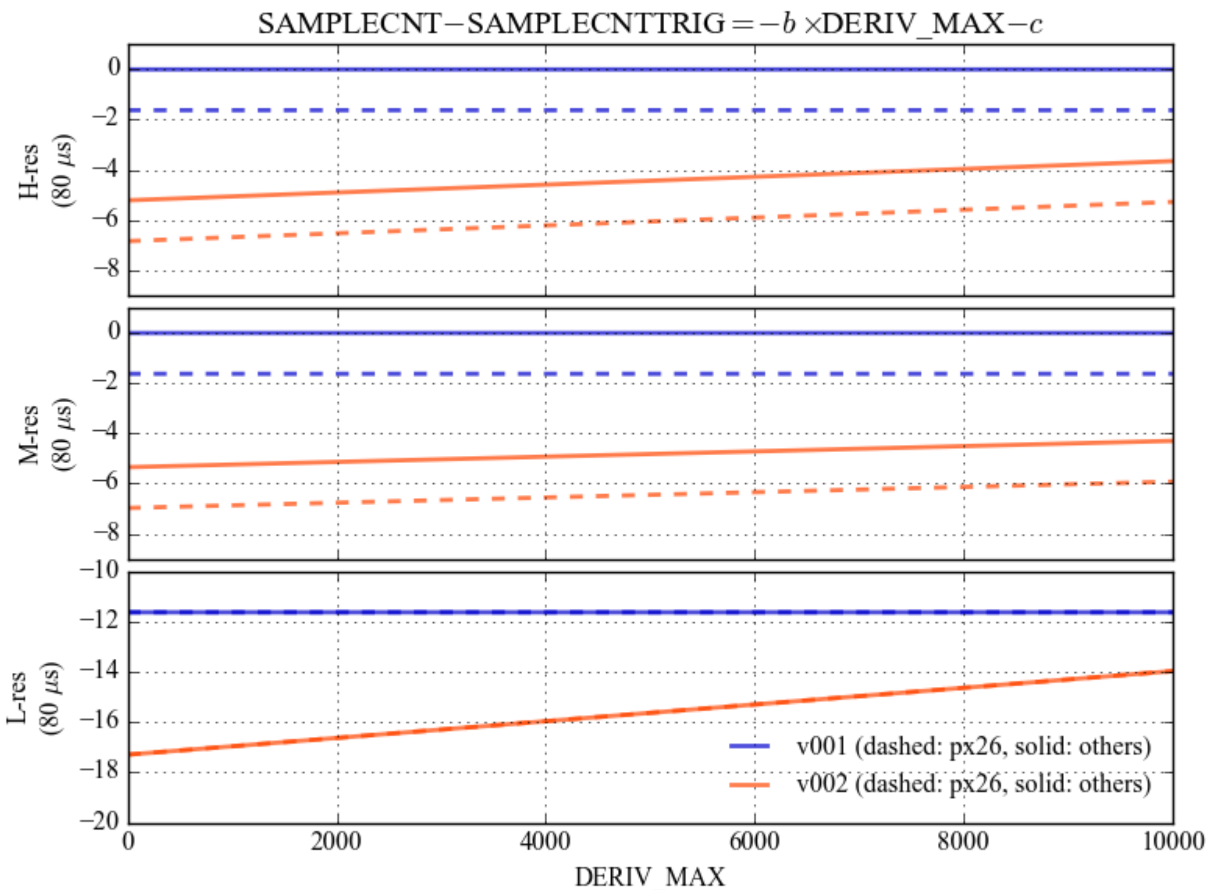
SAMPLECNT−SAMPLECNTTRIG = −b ×DERIV_MAX−c
H-res (80 μs)
M-res (80 μs)
L-res (80 μs)
v001 (dashed: px26, solid: others)
v002 (dashed: px26, solid: others)
DERIV_MAX
0
2000
4000
6000
8000
10000
0
−2
−4
−6
−8
−10
−12
−14
−16
−18
−20